Contents

List of Figures

1 Abstract

In the experiment, the dissociation energy $D_e = (405 \pm 14)\,1/\text{mm}$ and $E_{diss} = (1963 \pm 4)\,1/\text{mm}$ of a iodine molecule are calculated based on the absorption spectrum using Birges-Sponer plot. Furthermore the Morse potential for the excited state is calculated. A measurement of the emission spectrum did not provide useful information.

2 Theory

If a iodine molecule absorbs a photon, the energy gets absorbed. The energy of the molecule can be increased by

- a higher excited state of the electrons
- a higher vibration mode of the atom cores
- an increased rotation level.

For our experiment rotations are not relevant. As the cores are much heavier than the electrons around it, they react significantly slower to changes in the molecule. Therefore we can assume, that in short time scales, the electrons are the only part of the molecule that absorb energy.
The principle of slow cores and fast electrons are the reason we can make the Born-Oppenheimer approximation.

2.1 Born-Oppenheimer approximation

The Born-Oppenheimer approximation says that the wave function of the cores and the electrons can be split up for this reason

$$\psi(r_i, R_j) = \psi_{vib} \cdot \psi_k^0(r_i, R_j) \tag{1}$$

From the perspective of the electrons, the cores stand still and for the cores, the electron configuration stays a constant parameter.

2.2 Transitions in the experiment

In the experiment, the following transition of an iodine molecule should be observed

$$X^1\Sigma_{0,g}^+ \leftrightarrow B^3\Pi_{0,u}^+ \tag{2}$$

This means, that during the transition the projection of the total spin changes from 0 to 1. Usually this is a forbidden transition, because it hurts the selection rule $\Delta S = 0$. Due to strong spin-orbit interactions this rule

gets softened and the transition is possible.
Other transitions have only low intensities. That's why iodine is a useful molecule for this experiment.

2.3 Franck-Condon-principle

By increasing the excitement of the electrons, the potential of the molecule changes. Franck-Condon-principle gives information about how likely it is, that the vibration of cores transitions into a certain state. Using the Born-Oppenheimer approximation, the probability of a transition from one state to another is in bra ket notation

$$P = \langle \psi_{vib}\psi_{el}|\mu|\psi'_{vib}\psi'_{el}\rangle \tag{3}$$
$$\approx \langle \psi_{vib}|\psi'_{vib}\rangle \cdot \langle \psi_{el}|\mu_{el}|\psi'_{el}\rangle \tag{4}$$

μ is the dipole operator and μ_{el} the dipole operator of the electrons wave function.
The second scalar product shows if the transition is allowed or not. The first shows the overlap of vibration wave functions. This means, the more a vibration wave function in the excited state overlaps with the wave function the transition started from, the more likely it is to transit to this state.
This factor is also called Franck-Condon factor. The intensity of a transition is the square of P.
Each transition has a different energy difference between ground and excited state, which means that the wavelength of the emitted or absorbed light during the transition gives information about which transition happened.
Figure 1 shows the potential of different vibration modes at two different states of excitement for the electrons. On the x-axis is the distance between the cores and on the y-axis the energy.

2.4 Morse potential

The shape of the potential curve in figure 1 can be described with the approximation of a Morse potential. The Morse potential is given as

$$E_{pot}(R) = E_D \cdot \left(1 - e^{-a(R-R_e)}\right)^2 \tag{5}$$

and is shown in figure 2.
E_D is the dissociation energy which also is the asymptote in positive R direction. a is a constant that gives information about the stiffness of the core connection. R_0 is the distance between cores where their potential energy becomes minimal. For distances around R_e, the potential can be approximated with a parabola as well. The approximation gets worse for higher

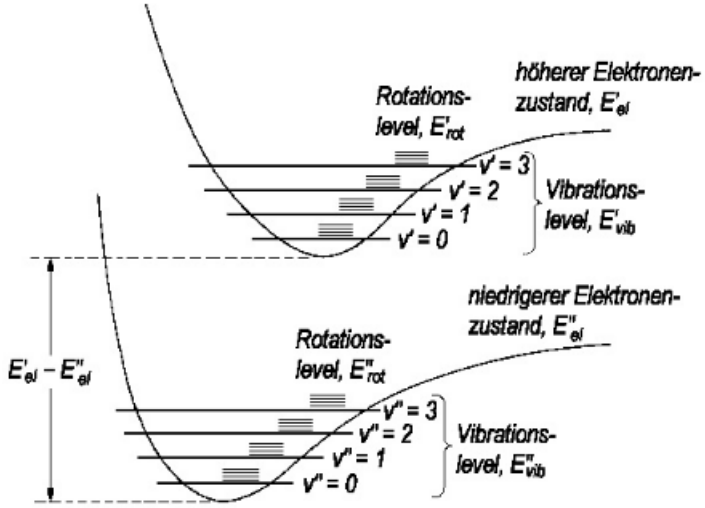

Figure 1: Energy levels of different molecule configurations

distances in both directions.
For high core distances the Morse potential is a better approximation. However for $R \to 0$, the Morse potential can become negative, whereas the real potential has a pole.
Using the morse potential, we can find an analytic solution for both the eigenfunction and the eigenvalue of the Schrödinger equation to our vibrational states. It is given as

$$E_{vib}(v) = \hbar\omega_e(v+\frac{1}{2}) - \hbar\omega_e x_e(v+\frac{1}{2})^2 \tag{6}$$

This is just the equation for an harmonic oscillator that got expanded by one more order.

2.5 Birge-Sponer plot

The energy of a photon is proportional to its frequency and therefore antiproportional to its wavelength. To be able to ignore proportionality constants like c or $\hbar$, G is used as a quantity of energy. It has the unit 1/m.
Using pertubation theory, we get

$$G(\nu) = \omega_e\left(\nu+\frac{1}{2}\right) - \omega_e x_e\left(\nu+\frac{1}{2}\right)^2 + ... \tag{7}$$

Higher orders can be ignored for our experiment. The lowest possible energy while ignoring higher orders is the energy where $\nu = 0$. The so called zero-point-energy is

$$G(0) = \frac{1}{2}\omega_e - \frac{1}{4}\omega_e x_e \tag{8}$$

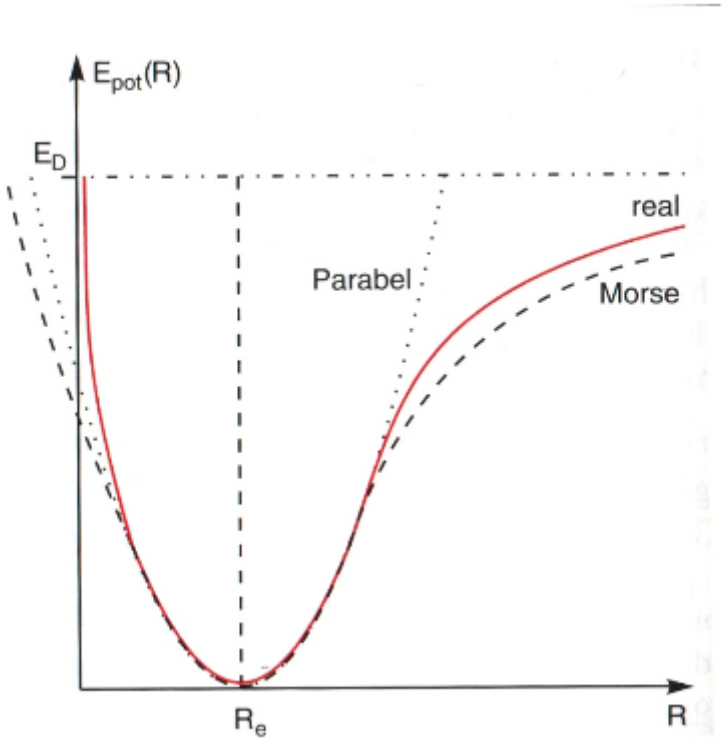

Figure 2: Parabola-, Morse- and real potential

The energy difference between two vibrational levels is then given as

$$\Delta G(\nu+\frac{1}{2}) := G(\nu+1) - G(\nu) = \omega_e - 2\omega_e x_e(\nu+1) \tag{9}$$

Since ν is discreet and there is a finite amount of different energy levels, we expect there to be a highest possible value for ν called ν_{diss}. At this value, $\Delta G(\nu+0,5) = 0$ since all states with higher energy are in the continuum. The energy needed to bring the molecule from $\nu = 0$ to ν_{diss} is called the dissociation energy D_0.

$$D_0 = \sum_{i=0}^{\nu_{diss}} \Delta G(\nu_i + \frac{1}{2}) \tag{10}$$

$$D_e = G(0) + D_0 \tag{11}$$

At the Birge-Sponer plot, $\Delta G(\nu+1/2)$ is visualized over $\nu+1/2$.
The cross section with the x-axis shows ν_diss. As shown in formular 9, the inclination is $a = -2\omega_e x_e$.
The y-intercept is $y_0 = \omega_e - \omega_e x_e$

Using the morse potential, the dissociation energy can be calculated directly as well. Therefore we calculate the minimum of $G(\nu)$ and set the derivation to zero. With the ν of the minimum, we get

$$D_e = \frac{\omega_e^2}{4\omega_e x_e} \tag{12}$$

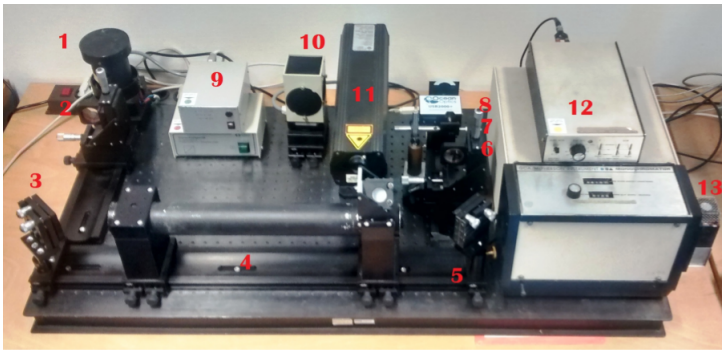

Abbildung 4: *Versuchsaufbau, 1: Halogenlampe, 2: Linse, 3: Spiegel, 4: Jod-Rohr, 5: Spiegel, 6: Linse, 7: Filter, 8: Spektrometer, 9: Netzgeräte für die Lampen, 10: Quecksilberdampflampe, 11: Helium-Neon-Laser, 12: Monochromator, 13: Photomultiplier*

Figure 3: Experimental Setup
1

3 Exeperimental Setup

For our iodine molecule, both the absorption and the emission spectrum should be detected.
For the absorption measurement a halogen lamp was used. With a lens the beam path was made parallel and send through a iodine tube. A second lense focused the light onto a spectrometer so that the filament was projected sharp in the detector.
To make more iodine molecules gaseous, the tube was heated with both a build in heater and an external advanced heating device.
For the emission measurement a He-Ne-Laser was used to bring iodine to an excited state. The emitted light was focused on a monochromator.
To calibrate the monochromator, a mercury vapour lamp was used.

4 Analysis

4.1 Detected Spectrum

The first measured absorption spectrum is shown in figure 4. To reduce the influence of statistical errors, the spectrum is the average of 27 measurements.

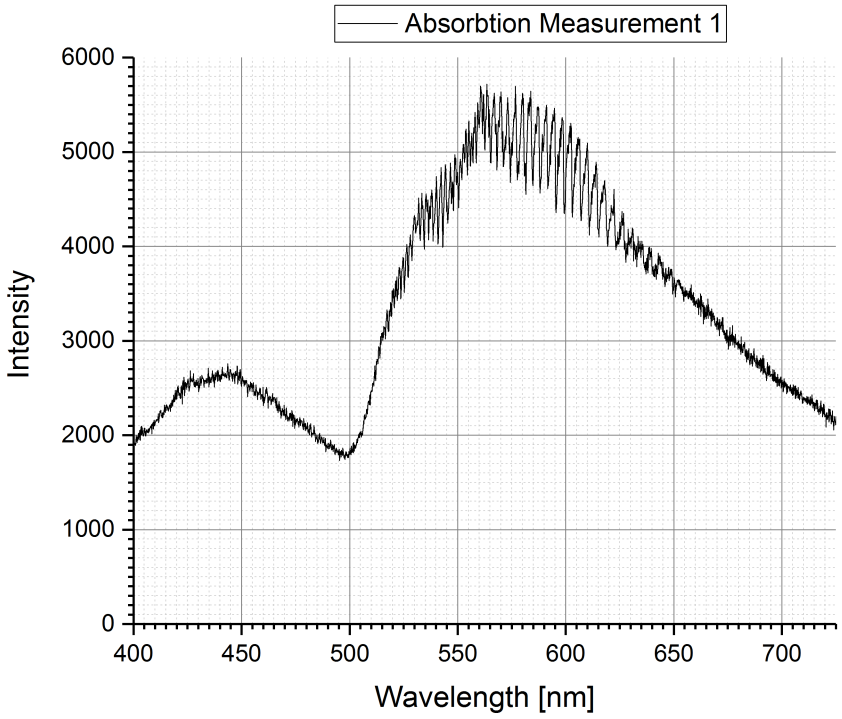

Figure 4: Spectrum of the first absorption measurement

For a wavelength of 500 nm or higher, the spectrum looks like it is expected. For lower wavelengths, there appeared an unexpected peak. Due to this peak, the beam path was refocused on the spectrometer and a second spectrum was measured. This spectrum is shown in figure 5. As one can see, the measured intensities are a lot higher and the peaks are sharper. This shows, that the beam is better focused now. However, for low wavelengths, there is still an unexpected peak and a minimum.
Minima in the spectrum stand for energy that got absorbed by the iodine molecule. To see if the shape of the spectrum for wavelengths smaller than 500 nm is created by the iodine molecule, the spectrum of the halogen lamp without the iodine tube was measured as well. It is shown in figure 6. The

total intensities are lower because of a different beam path. Still, it shows, that the peak and the minimum are created by the iodine tube.
For the further analysis, the second absorbtion measurement is the one, that is worked with.

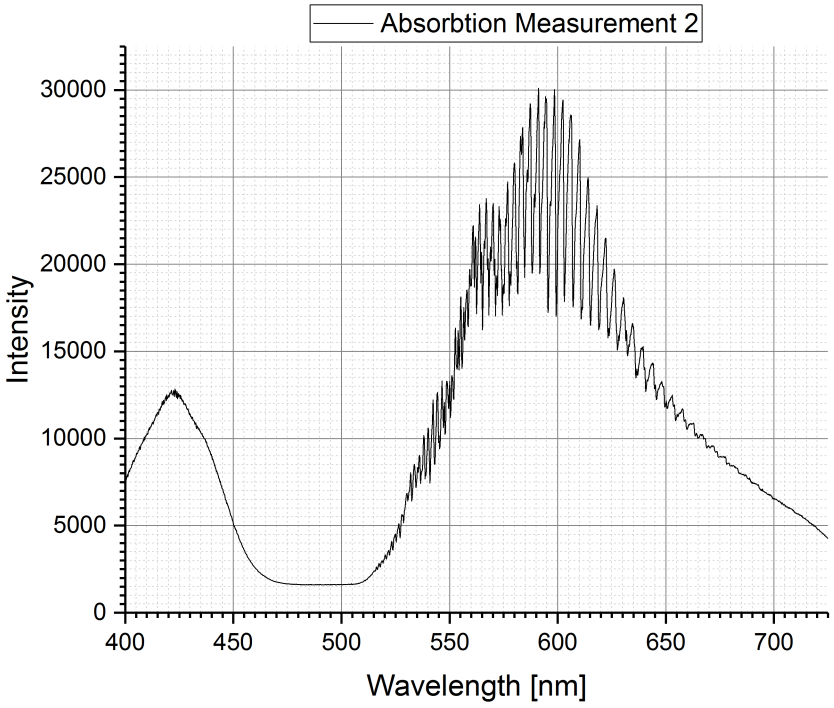

Figure 5: Spectrum of the second absorption measurement

In the instruction paper was a hint, that the absorption line of the transition $\nu'' = 0 \rightarrow \nu' = 25$ as at a wavelength of 545,8 nm. This absorption line was identified at $\lambda = 545{,}4$ nm. To have a closer look at the minima, the spectrum in range from 495 to 635 nm is shown in the figures 10 - 16 in steps of 20 nm.
A minimum at a shorter wavelength in the spectrum means, that more energy was used for the transition. Therefore the value of ν' is higher. To make sure, only minima of a transition starting at $\nu'' = 0$ are marked, $\Delta\lambda = \lambda(\nu) - \lambda(\nu+1)$ is calculated. For two neighboured minima it should be around the same size with a tendency to get smaller for smaller wavelenths. The wavelengths λ of the minima, $\Delta\lambda$ and ν' are shown in tabular 6.

For finding transitions starting at ν' =1 or 2, it was used that $\Delta\lambda$ had the same value independently from which ν'' the transition started. The

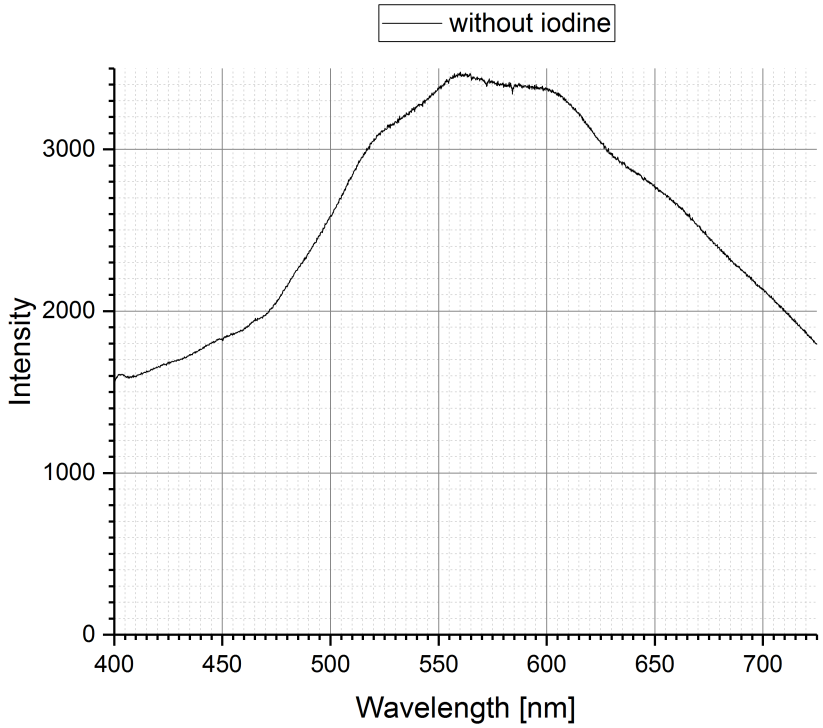

Figure 6: First absorption measurement

positions of the minima for $\nu'' = 1;2$ can also be found in table 6. The uncertainty on the position of a minimum is $s_\lambda = 0,1$ nm. For $\Delta\lambda$ it is therefore $s_{\Delta\lambda} = \sqrt{2} \cdot s_\lambda = \sqrt{2} \cdot 0,1$ nm

4.2 Birge-Sponer plot

To be able to plot $\Delta G(\nu + 1/2)$ on $\nu + 1/2$, the reciprocal values k of the wavelength are calculated and subtracted from each other

$$k(\nu') = \frac{1}{\lambda(\nu')} \qquad s_{k(\nu')} = \frac{s_\lambda}{\lambda(\nu')^2} \tag{13}$$

$$\Delta G(\nu' + 1/2) = k(\nu') - k(\nu' + 1) \qquad s_{\Delta G} = \sqrt{s^2_{k(\nu')} + s^2_{k(\nu'+1)}} \tag{14}$$

The calculated values for the ΔG of all three ν'' can be found in tables 7 - 9

4.2.1 Results of the linear regression

For the Birges-Sponer plot of this data, a linear regression was made. The fitting results are shown in table 1

ν''	a	s_a	y_0	s_{y_0}
0	-0,208	0,007	13,2	0,2
1	-0,19	0,02	12,7	0,4
2	-0,177	0,012	12,29	0,14

Table 1: Results of the three Birges-Sponer plots.

As it was already discussed in part 2.5, ω_e and $\omega_e x_e$ can be calculated from the inclination a and the y-offset y_0.

$$\omega_e x_e = -\frac{a}{2} \qquad s_{\omega_e x_e} = \frac{s_a}{2} \tag{15}$$

$$\omega_e = y_0 - \frac{a}{2} \qquad s_{\omega_e} = \sqrt{s_{y_0}^2 + (\frac{s_a}{2})^2} \tag{16}$$

The calculated values for ω_e and $\omega_e x_e$ can be found in table 2

ν''	$\omega_e x_e$ / 1/mm	$s_{\omega_e x_e}$ / 1/mm	ω / 1/mm	s_ω / 1/mm
0	0,104	0,004	13,3	0,2
1	0,096	0,010	12,8	0,4
2	0,088	0,006	12,38	0,15

Table 2: Calculated values for ω_e and $\omega_e x_e$

4.2.2 Weightened averages

For all three measurement series, it is expected to receive the same results for a, y_0, ω_e and $\omega_e x_e$. That's why one can calculate the wheigtened average of those values to reduce the uncertainty. The formula for the wheigtened average is given as

$$\bar{a} = \frac{\sum_{i=0}^{3}(a_i/s_i^2)}{\sum_{i=0}^{3}(1/s_i)^2} \tag{17}$$

$$s_{\bar{a}} = \frac{1}{\sqrt{\sum_{i=0}^{3}(1/s_i)^2}} \tag{18}$$

The calculated values can be found in table 3

The highest possible ν' that is still bound in the potential can be calculated by looking at the cross section with the x axis. Therefore ΔG is set

quantity	weighted average / 1/mm	uncertainty / 1/mm
a	-0,199	0,006
y_0	12,623	0,112
$\omega_e x_e$	0,100	0,003
ω_e	12,72	0,11

Table 3: calculated weightened averages

to 0. Quantities marked with a bar are the averages.

$$0 = \Delta G(\nu_{diss} + 1/2) = y_0 + a(\nu_{diss} + 1/2) \tag{19}$$

$$\nu_{diss} = -\frac{\bar{y_0}}{\bar{a}} - 1/2 \tag{20}$$

$$s_{\nu_{diss}} = \frac{\bar{y_0}}{\bar{a}} \sqrt{\left(\frac{s_a}{a}\right)^2 + \left(\frac{s_{y_0}}{y_0}\right)^2} \tag{21}$$

Like this, we get

$$\boxed{\nu_{diss} = 62,8 \pm 1,9} \tag{22}$$

4.2.3 Solving the sum for D_0

To get the dissociation energy D_0, the sum, given in equation 10 has to be solved. It can be used that a lot of terms cancel each other out, so that the remaining sum looks as follows

$$D_0 = \sum_{i=0}^{\nu_{diss}} \Delta G(\nu_i + \frac{1}{2}) = \sum_{i=0}^{\nu_{diss}} G(\nu_i + 1) - G(\nu_i) \tag{23}$$

$$= \sum_{i=0}^{\nu_{diss}} \omega_e \left(\nu_i + \frac{3}{2}\right) - \omega_e x_e \left(\nu_i + \frac{3}{2}\right)^2 - \omega_e \left(\nu_i + \frac{1}{2}\right) + \omega_e x_e \left(\nu_i + \frac{1}{2}\right)^2 \tag{24}$$

$$= \omega_e \left(\frac{3}{2}\right) - \omega_e x_e \left(\frac{3}{2}\right)^2 - \omega_e \left(\frac{1}{2}\right) + \omega_e x_e \left(\frac{1}{2}\right)^2 \tag{25}$$

$$+ \omega_e \left(\frac{5}{2}\right) - \omega_e x_e \left(\frac{5}{2}\right)^2 - \omega_e \left(\frac{3}{2}\right) + \omega_e x_e \left(\frac{3}{2}\right)^2 \tag{26}$$

$$+ ... \tag{27}$$

$$+ \omega_e \left(\nu_{diss} + \frac{3}{2}\right) - \omega_e x_e \left(\nu_{diss} + \frac{3}{2}\right)^2 - \omega_e \left(\nu_{diss} + \frac{1}{2}\right) + \omega_e x_e \left(\nu_{diss} + \frac{1}{2}\right)^2 \tag{28}$$

$$= \omega_e \left(\nu_{diss} + \frac{3}{2}\right) - \omega_e x_e \left(\nu_{diss} + \frac{3}{2}\right)^2 - \frac{1}{2}\omega_e + \frac{1}{4}\omega_e x_e \tag{29}$$

Here it is used that the two last summands of each line were exactly the negative of the first two summands of the line above.

Interestingly, one can see, that the last two summands of the final result are just the zero point energy that got substracted by the rest. This means the first two summands are just D_e
This leaves us with an expression for the dissociation energy, that is just

$$D_0 = \omega_e(\nu_{diss}+1) - \omega_e x_e\left(\nu_{diss}^2+2+3\nu_{diss}\right) \tag{30}$$

The uncertainty can then be calculated by error propagation as

$$s_{D_0} = \sqrt{((\nu_{diss}+1)s_{\omega_e})^2 + ((\nu_{diss}^2+2+3\nu_{diss})\,s_{\omega_e x_e})^2 + ((\omega_e - 2\omega_e x_e \nu_{diss} + 3\omega_e x_e)s_{\nu_{diss}})^2} \tag{31}$$

$$\boxed{D_0 = (399 \pm 14)\,1/\mathrm{mm}} \tag{32}$$

The zero point energy G(0) can be calculated as in formula 8

$$G(0) = \frac{1}{2}\omega_e - \frac{1}{4}\omega_e x_e \tag{33}$$

$$s_{G(0)} = \sqrt{\left(\frac{1}{2}s_{\omega_e}\right)^2 + \left(\frac{1}{4}s_{\omega_e x_e}\right)^2} \tag{34}$$

And is

$$\boxed{G(0) = (6{,}33 \pm 0{,}06)\,1/\mathrm{mm}} \tag{35}$$

The dissociation energy D_e can therefore be calculated as

$$D_e = D_0 + G(0) \tag{36}$$

$$s_{D_e} = \sqrt{s_{D_0}^2 + s_{G(0)}^2} \tag{37}$$

and is

$$\boxed{D_e = (405 \pm 14)\,1/\mathrm{mm}} \tag{38}$$

4.2.4 Dissociation energy D_e with the Morse potential

Like in formula 12, the dissociation energy D_e can be calculated as follows, using the approximation of a Morse potential

$$D_{e,Morse} = \frac{\omega_e^2}{4\omega_e x_e} \tag{39}$$

$$s_{D_e} = D_{e,Morse}\sqrt{\left(2\frac{s_{\omega_e}}{\omega_e}\right)^2 + \left(\frac{s_{\omega_e x_e}}{\omega_e x_e}\right)^2} \tag{40}$$

It is

$$\boxed{D_{e,Morse} = (405 \pm 14)\,1/\mathrm{mm}} \tag{41}$$

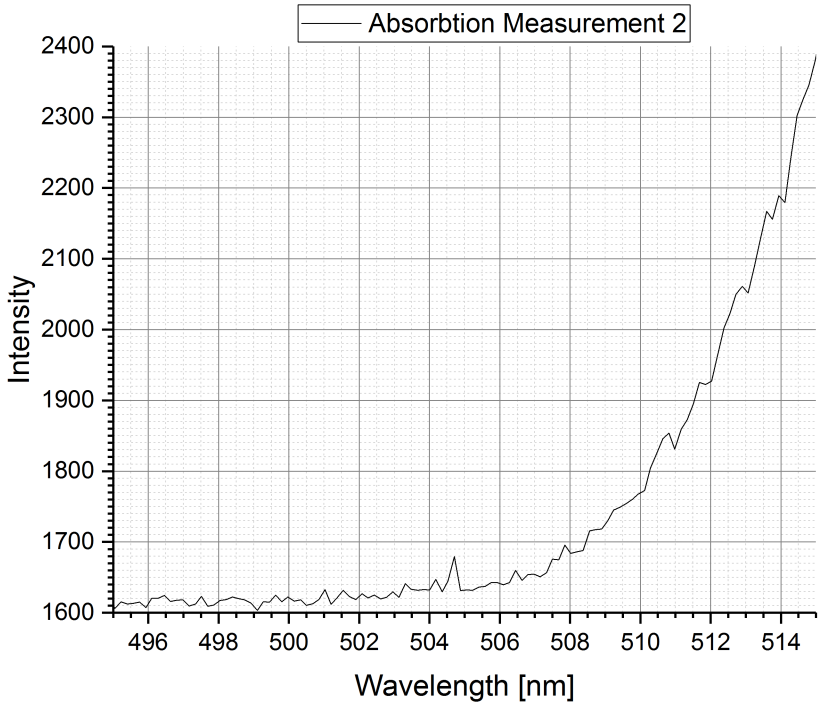

Figure 7: Spectrum from 495-515nm

4.3 Dissociation Energy E_{diss}

To calculate the Dissociation Energy E_{diss} the beginning of the measured absorption spectrum is used. There the lowest wavelength which was absorbed during the experiment can be found. In other words, the lowest absorbed wavelength is proportional to the maximum energy that can be absorbed by the molecule before the electron is leaving it. Thus, in figure 10 the minimum wavelength can be estimated to be $\lambda_{min} = (509 \pm 1)\text{nm}$.

The line at $\lambda = 545,8\text{nm}$ corresponds to the transition from $\nu'' = 0 \rightarrow \nu' = 15$. In the measurements the closest line is at $\lambda = 545,4\text{nm}$ (**??**). Thus, there is a displacement wavelength of $\lambda_{disp} = (0,4 \pm 0,1)\text{nm}$. As this error is comparatively small it is negligible. The Dissociation Energy follows as

$$E_{diss} = \frac{1}{\lambda_{min} + \lambda_{displ}} = 1963,094 \frac{1}{\text{mm}} \tag{42}$$

$$s_{E_{diss}} = \frac{s_{\lambda_{min}}}{(\lambda_{min} + \lambda_{displ})^2} = 3,85 \frac{1}{\text{mm}} \tag{43}$$

Therefore the final result for the Dissociation Energy is

$$\boxed{E_{diss} = (1963 \pm 4)\frac{1}{\text{mm}}} \tag{44}$$

4.4 Excitation Energy T_e

The excitation energy is the energy difference between the excited state and the ground state of a system. In this experiment it is computable by

$$T_e = E_{diss} - D_0 \tag{45}$$

$$s_{T_e} = \sqrt{(s_{diss})^2 + (s_{D_0})^2} \tag{46}$$

The result is

$$\boxed{T_e = (1564 \pm 15)\frac{1}{\text{mm}}} \tag{47}$$

4.5 Morse Potential of the Excited State

Given in 1 is the formula for the Morse potential.

$$E_{pot} = D_E \cdot (1 - \exp(-a(R - R_e))^2 \tag{48}$$

Before, $D_E = (405 \pm 14)\frac{1}{\text{mm}}$ was determined. $R_e = 2,979$Åis given in 2 and a can be determined by using

$$a = \sqrt{\frac{\omega_e x_e 4\pi c \mu}{\hbar}} \tag{49}$$

where μ is the reduced mass of the iodine molecule.

$$s_a = \frac{a}{2\omega_e x_e} \cdot s_{\omega_e x_e} \tag{50}$$

The result is

$$\boxed{a = (1,941 \pm 0,03)\frac{1}{\text{Å}}} \tag{51}$$

The resulting Morse Potential can be seen in 8.

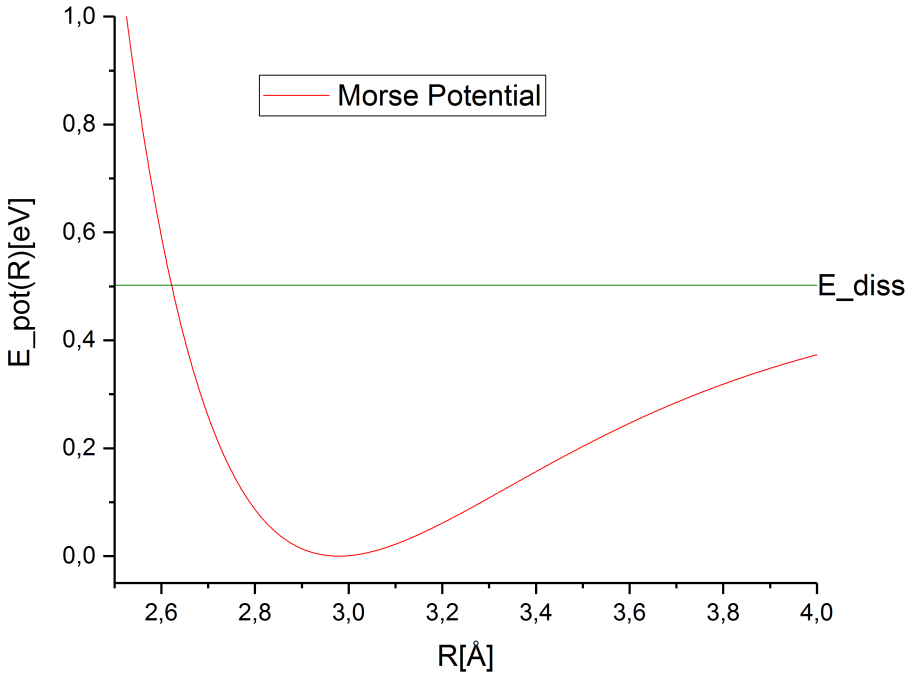

Figure 8: Morse Potential

5 Emission

Before measuring the emission pattern, the monochromator has to be calibrated. Therefore the halogene lamp is exchanged with a mercury lamp. The emission spectrum of mercury is known, thus it is possible to find the correct position of the emission lines on the scale. The detected peaks can be seen in 9.
Obviously the detected pattern does not fit with the pattern that is expected for a mercury lamp. The amount of peaks is too large to be caused by the mercury lamp. It was tried in several measurements to exclude the source of irritation from the experiment. The light in the room is switched of, the entrance of the monochromator is covered, all light sources which could possibly interfere with the experiment are tried to be eliminated as good as possible. Also, the iodine tube is heated up more with a hairdryer to have more iodine molecules in gasiform. Still, the monochromator measures those peaks which appear on random position in the spectrum. Taking a closer look on the measurement devices, the discriminator is seen to measure random signals. Those signals seem to be correlated with measured peaks

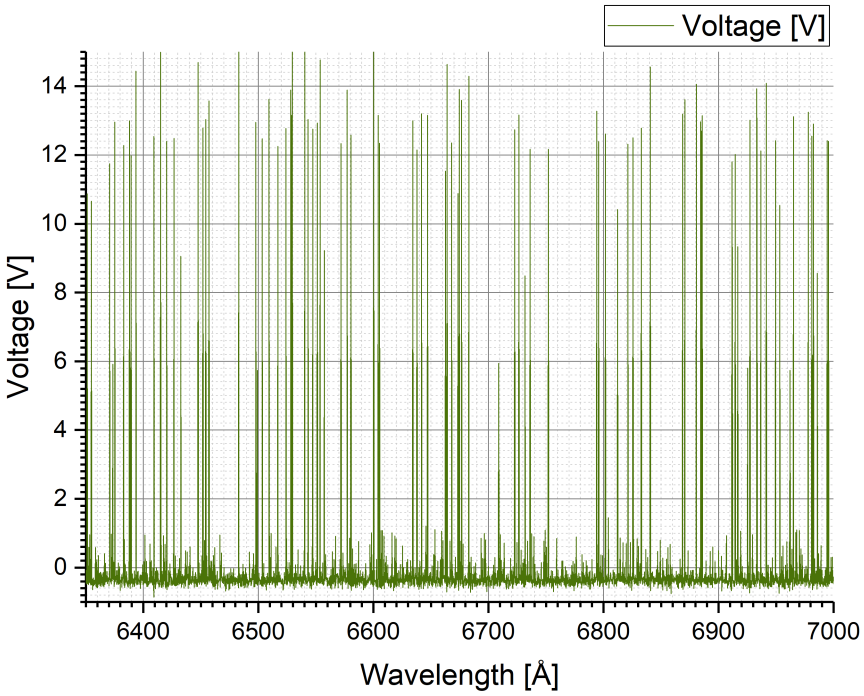

Figure 9: Calibration

in the picture.
As there is a systematic problem with the monochromator, it is impossible to continue the experiment for the emission spectrum of the iodine molecule. The background noise is to strong and the signal of the mercury lamp which is searched during this setup is impossible to detect and extract from the background measurements.

6 Discussion

6.1 Absorption

6.1.1 Detected spectrum

For wavelengths greater than 500 nm, the absorption spectrum of the iodine molecule looked like it was expected. However for smaller wavelengths (460 nm -500 nm), there is a minimum that can not be explained by the absorption properties of iodine. As it was shown, the minimum disappeared when removing the iodine tube.
Therefore it is likely, that it was created by diffraction effects on the tube. It is difficult to name a specific object in the tube, because there is no information about how it looks on the inside of the tube.
Before heating up the pipe, it was noticed, that iodine crystallised on the windows of the tube. With a melting point of 113,70°C [3], it is very likely that there was even after heating still solid iodine in the tube. This could be a source of diffraction as well.

6.1.2 Vibrational constants $\omega_e x$ and ω_e

With the help of Birge-Sponer plot, the vibrational constants $\omega_e x_e$ and ω_e were calculated for transitions starting at $\nu'' = 0; 1$ and 2. They are summarised in tabular 4

ν''	$\omega_e x_e$ / 1/mm	ω / 1/mm
0	0,104 ± 0,004	13,3 ± 0,2
1	0,096 ± 0,010	12,8 ± 0,4
2	0,088 ± 0,006	12,38 ± 0,15

Table 4: Summary of measured values for ω_e and $\omega_e x_e$

For $\nu'' = 0$ and $\nu'' = 1$, the constants are in range of at least 2 standard deviations of each other.
For $\nu'' = 2$, $\omega_e x_e$ is in the range of 2 standard deviations of the value for $\nu'' = 1$ as well. In comparison to $\nu'' = 0$, both $\omega_e x$ and ω_e are significantly smaller, even though the statistical uncertainty isn't notably bigger. The reason for this systematic offset is very likely to be found in the numeration of minima for $\nu'' = 2$. As it is shown in table 6, it is not clear where the numeration of peaks has to start to match with the values for $\Delta\lambda$ for the series with $\nu'' = 0$.
In table 5, the wheightened averages of all the measured values are compared to the literature values of the National Institute for Standards and Technology (NIST)[4]. The values from the experiment are in the same magnitude as the literature values, but vary a lot in perspective of the standard deviation. Especially quantities that were directly calculated from the

Quantity	experimental value	literature value	variation
$\omega_e x_e$ / 1/cm	100 ± 3	$125,96$	9 σ
ω_e / 1/cm	$1,272 \pm 0,011$	$0,764$	45 σ
D_e (Birge) / 1/cm	4050 ± 140	4391	3 σ
D_e (Morse) / 1/cm	4050 ± 140	4391	3 σ
E_{diss} / 1/cm	19630 ± 40	20014	10 σ
T_e / 1/cm	15640 ± 150	15769	1 σ

Table 5: Comparison between measured results and literature values.

Birge-Sponer plot like $\omega_e x_e$ and ω_e have high variations. This might be due to the relatively small error of $s_\lambda = 0,1$ nm that was raised on the position of the minima in the intensity distribution.
As a reading error, this uncertainty seems legit, but it has to be considered, that the measured distribution was only the average distribution over 27 measurement series. Statistical fluctuation can still have shifted minima to slightly different wavelengths. Therefore the measured intensity disribution underlies a statistical error itself that did not influence the error propagation. The real statistical uncertainty is probably bigger.
The calculated values for D_e and T_e did match well with the literature values. Interestingly, both ways to calculate the dissociation energy delivered in regard of their uncertainties the same result.
The highest possible vibrational state from the Birge-Sponer plot is

$$\boxed{\nu'_{diss} = 62,8 \pm 1,9} \tag{52}$$

As ν has to be a whole number, this would usually mean, that the highest possible configuration, is $\nu'_{diss} = 62$ because all higher values are not bound in the potential anymore. Due to the relatively high uncertainty $\nu'_{diss} = 63$ is more likely to fit.

6.2 Emission

As it was already mentioned in the execution part of the protocol, it was not possible to take any qualified measurements for the emission spectrum of the iodine molecule. Even after all the possible improvements were made, it was still not possible to detect a reasonable signal with the device. All the lights in the room were switched off to reduce the light pollution in the experiment as the spectrometer is really sensitive even to small amounts of light. After discovering that there is a huge background noise which is detected by the spectrometer, the entrance of it was covered, thus it was expected to detect no signal at all as no light should enter the device. Regardless a strong signal with random peaks was detected. Therefore the conclusion is, that the problem lies inside of the detector and became irresolvable.

It was also tried to intensify the given signal of the iodine molecule by heating up the tube next to the already built in heater. A hairdryer was used to especially heaten up the glass of the entrance of the tube which foggened up if it cooled down. To take the measurements it was waited until the small plate which was hanging on the entrance glass fell down and the glass was clear again. Still, the detected signal was not strong enough to be separated from the interfering background noise.

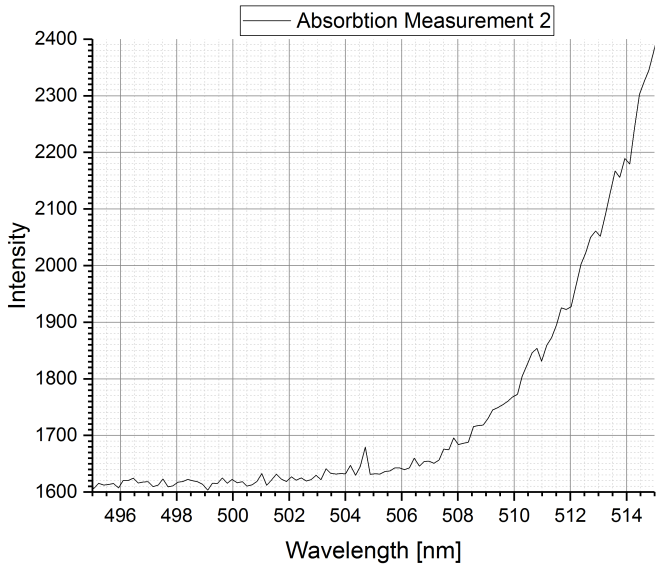

Figure 10: 495-515nm

7 Appendix

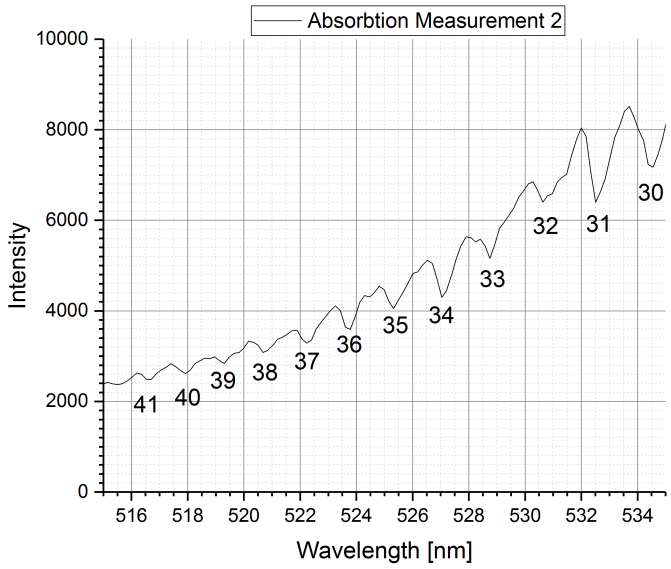

Figure 11: Absorption spectrum for 515-535nm.

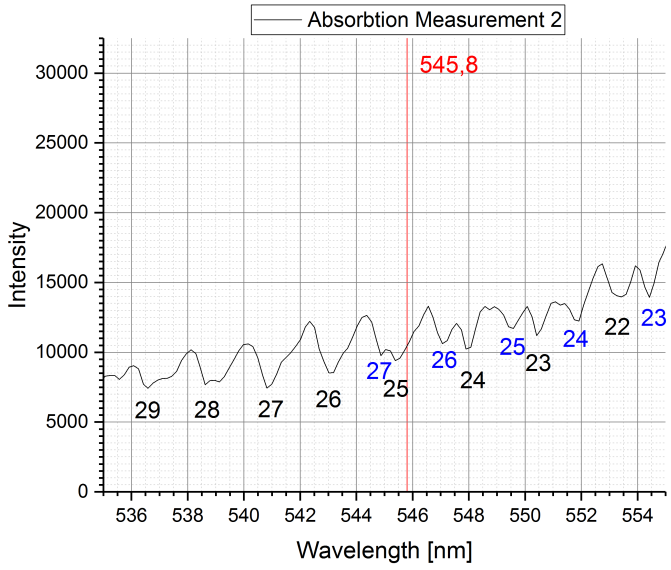

Figure 12: Absorption spectrum for 535-555nm

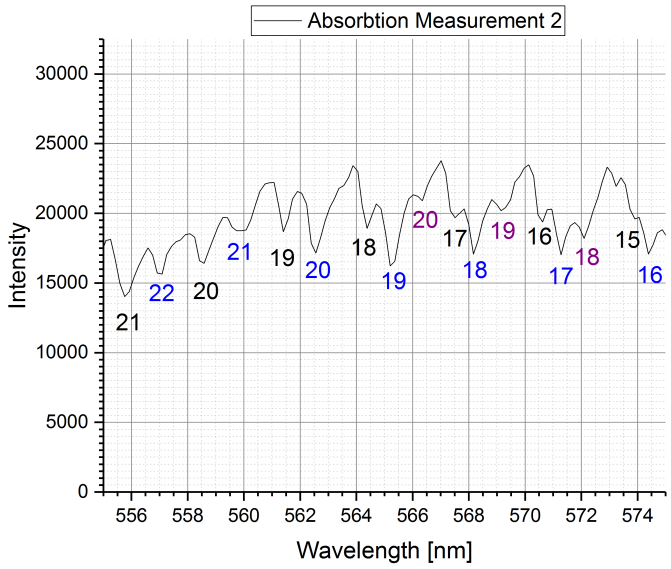

Figure 13: Absorption spectrum for 555-575nm

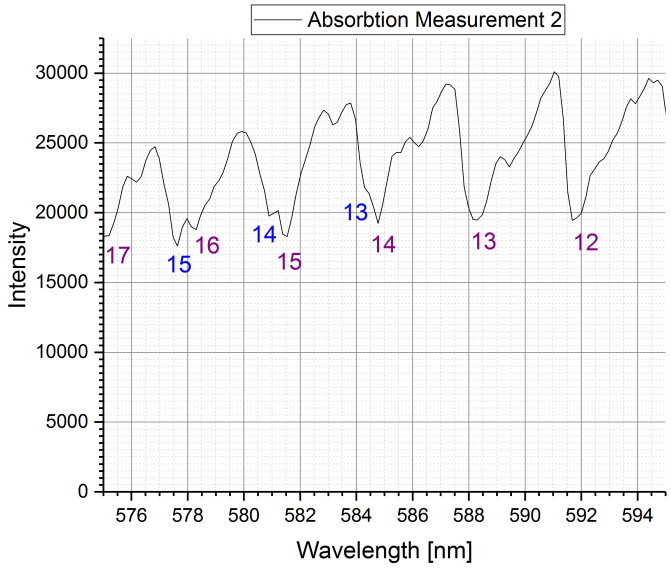

Figure 14: Absorption spectrum for 575-595nm

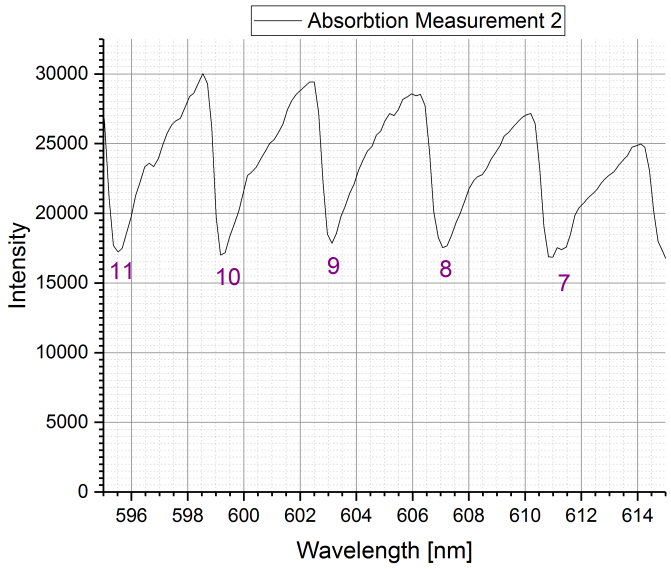

Figure 15: Absorption spectrum for 595-615nm

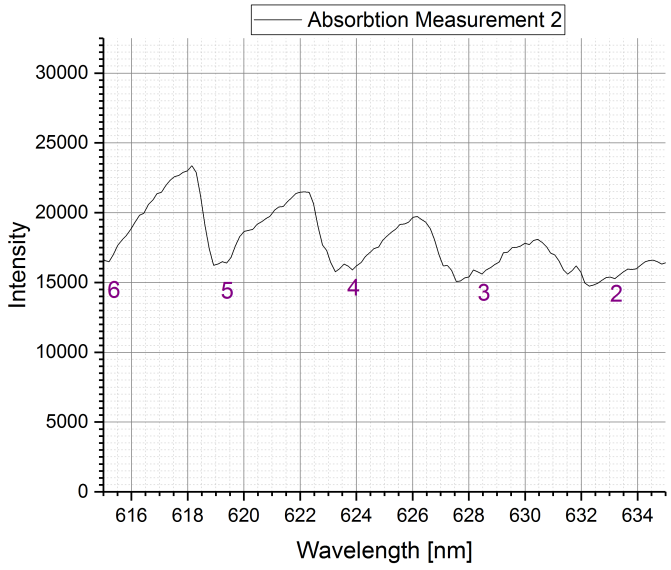

Figure 16: Absorption spectrum for 615-635nm

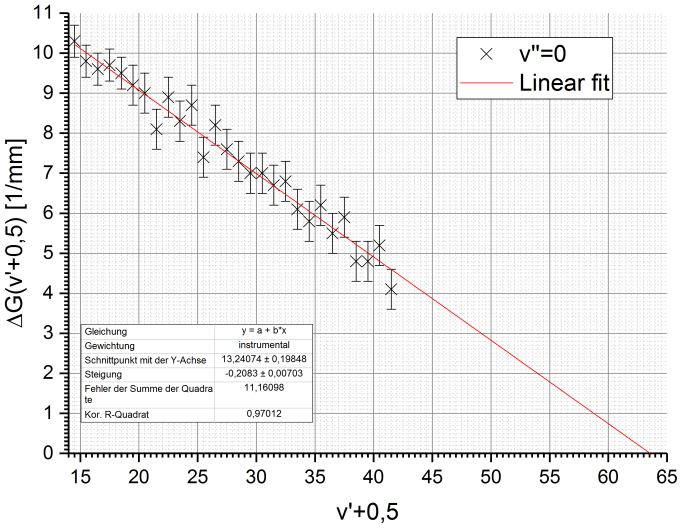

Figure 17: Birge-Sponer plot for $\nu'' = 0$

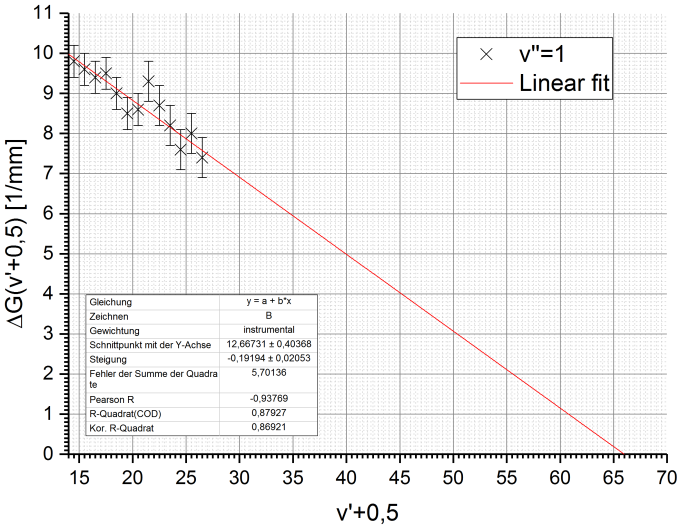

Figure 18: Birge-Sponer plot for $\nu'' = 1$

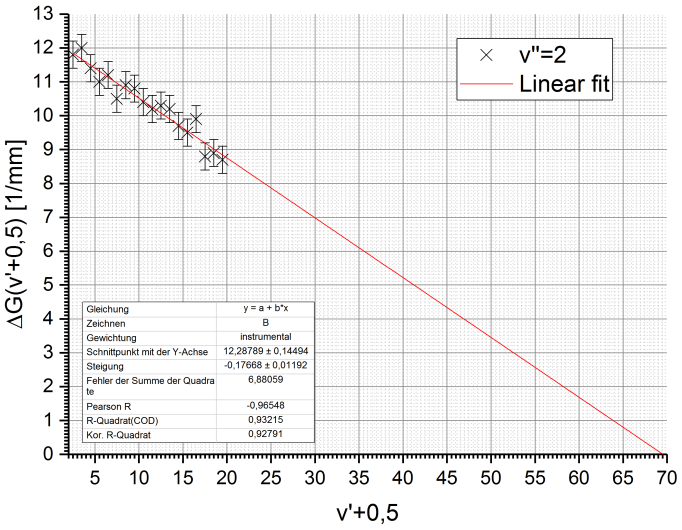

Figure 19: Birge-Sponer plot for $\nu'' = 2$

References

[1] [instructions]
Instruction paper published at `http://omnibus.uni-freiburg.de/~phypra/fp/Versuche/FP1/FP1-16-J2-Molekuel/` 12.09.2017 13:51

[2] [exam paper]
Martine Meyer: "Verbesserung des Versuchs Spektroskopie am J2-Molekul des Fortgeschrittenen Praktikums" published at `http://omnibus.uni-freiburg.de/~phypra/fp/Versuche/FP1/FP1-16-J2-Molekuel/` 12.09.2017 13:51

[3] [chem.]
http://www.chemie.de/lexikon/Iod.html

[4] [NIST]
http://webbook.nist.gov/cgi/cbook.cgi?ID=C7553562Mask=1000

ν'	$\nu'' = 0$		$\nu'' = 1$		$\nu'' = 2$	
	λ / nm	$\Delta\lambda$ / nm	λ / nm	$\Delta\lambda$ / nm	λ / nm	$\Delta\lambda$ / nm
1						
2					633,2	4,7
3					628,5	4,7
4					623,8	4,4
5					619,4	4,2
6					615,2	4,2
7					611	3,9
8					607,1	4
9					603,1	3,9
10					599,2	3,7
11					595,5	3,6
12					591,9	3,6
13			584,4	3,5	588,3	3,5
14	577,2	3,4	580,9	3,3	584,8	3,3
15	573,8	3,2	577,6	3,2	581,5	3,2
16	570,6	3,1	574,4	3,1	578,3	3,3
17	567,5	3,1	571,3	3,1	575	2,9
18	564,4	3	568,2	2,9	572,1	2,9
19	561,4	2,9	565,3	2,7	569,2	2,8
20	558,5	2,8	562,6	2,7	566,4	
21	555,7	2,5	559,9	2,9		
22	553,2	2,7	557	2,7		
23	550,5	2,5	554,3	2,5		
24	548	2,6	551,8	2,3		
25	545,4	2,2	549,5	2,4		
26	543,2	2,4	547,1	2,2		
27	540,8	2,2	544,9			
28	538,6	2,1				
29	536,5	2				
30	534,5	2				
31	532,5	1,9				
32	530,6	1,9				
33	528,7	1,7				
34	527	1,6				
35	525,4	1,7				
36	523,7	1,5				
37	522,2	1,6				
38	520,6	1,3				
39	519,3	1,3				
40	518	1,4				
41	516,6	1,1				
42	515,5					

Table 6: Location of transitions starting from ν''=0;1;2 to ν' in the spectrum

ν'	$\nu'+1/2$	λ /nm	s_λ / nm	k / 1/mm	s_k /1/mm	$G(\nu'+0,5)$ / 1/mm	s_G / 1/mm
14	14,5	577,2	0,1	1732,5	0,3	10,3	0,4
15	15,5	573,8	0,1	1742,8	0,3	9,8	0,4
16	16,5	570,6	0,1	1752,5	0,3	9,6	0,4
17	17,5	567,5	0,1	1762,1	0,3	9,7	0,4
18	18,5	564,4	0,1	1771,8	0,3	9,5	0,4
19	19,5	561,4	0,1	1781,3	0,3	9,2	0,5
20	20,5	558,5	0,1	1790,5	0,3	9,0	0,5
21	21,5	555,7	0,1	1799,5	0,3	8,1	0,5
22	22,5	553,2	0,1	1807,7	0,3	8,9	0,5
23	23,5	550,5	0,1	1816,5	0,3	8,3	0,5
24	24,5	548	0,1	1824,8	0,3	8,7	0,5
25	25,5	545,4	0,1	1833,5	0,3	7,4	0,5
26	26,5	543,2	0,1	1840,9	0,3	8,2	0,5
27	27,5	540,8	0,1	1849,1	0,3	7,6	0,5
28	28,5	538,6	0,1	1856,7	0,3	7,3	0,5
29	29,5	536,5	0,1	1863,9	0,3	7,0	0,5
30	30,5	534,5	0,1	1870,9	0,4	7,0	0,5
31	31,5	532,5	0,1	1877,9	0,4	6,7	0,5
32	32,5	530,6	0,1	1884,7	0,4	6,8	0,5
33	33,5	528,7	0,1	1891,4	0,4	6,1	0,5
34	34,5	527	0,1	1897,5	0,4	5,8	0,5
35	35,5	525,4	0,1	1903,3	0,4	6,2	0,5
36	36,5	523,7	0,1	1909,5	0,4	5,5	0,5
37	37,5	522,2	0,1	1915,0	0,4	5,9	0,5
38	38,5	520,6	0,1	1920,9	0,4	4,8	0,5
39	39,5	519,3	0,1	1925,7	0,4	4,8	0,5
40	40,5	518	0,1	1930,5	0,4	5,2	0,5
41	41,5	516,6	0,1	1935,7	0,4	4,1	0,5
42	42,5	515,5	0,1	1939,9	0,4		

Table 7: Calculated values and uncertainties of ΔG for ν''=0

ν'	$\nu'+1/2$	λ /nm	s_λ / nm	k / 1/mm	s_k /1/mm	$G(\nu'+0,5)$ / 1/mm	s_G / 1/mm
13	13,5	584,4	0,1	1711,2	0,3	10,3	0,4
14	14,5	580,9	0,1	1721,5	0,3	9,8	0,4
15	15,5	577,6	0,1	1731,3	0,3	9,6	0,4
16	16,5	574,4	0,1	1740,9	0,3	9,4	0,4
17	17,5	571,3	0,1	1750,4	0,3	9,5	0,4
18	18,5	568,2	0,1	1759,9	0,3	9,0	0,4
19	19,5	565,3	0,1	1769,0	0,3	8,5	0,4
20	20,5	562,6	0,1	1777,5	0,3	8,6	0,4
21	21,5	559,9	0,1	1786,0	0,3	9,3	0,5
22	22,5	557	0,1	1795,3	0,3	8,7	0,5
23	23,5	554,3	0,1	1804,1	0,3	8,2	0,5
24	24,5	551,8	0,1	1812,3	0,3	7,6	0,5
25	25,5	549,5	0,1	1819,8	0,3	8,0	0,5
26	26,5	547,1	0,1	1827,8	0,3	7,4	0,5
27	27,5	544,9	0,1	1835,2	0,3		

Table 8: Calculated values and uncertainties of ΔG for ν''=1

ν'	$\nu'+1/2$	λ /nm	s_λ / nm	k / 1/mm	s_k /1/mm	$G(\nu'+0,5)$ / 1/mm	s_G / 1/mm
2	2,5	633,2	0,1	1579,3	0,2	11,8	0,4
3	3,5	628,5	0,1	1591,1	0,3	12,0	0,4
4	4,5	623,8	0,1	1603,1	0,3	11,4	0,4
5	5,5	619,4	0,1	1614,5	0,3	11,0	0,4
6	6,5	615,2	0,1	1625,5	0,3	11,2	0,4
7	7,5	611	0,1	1636,7	0,3	10,5	0,4
8	8,5	607,1	0,1	1647,2	0,3	10,9	0,4
9	9,5	603,1	0,1	1658,1	0,3	10,8	0,4
10	10,5	599,2	0,1	1668,9	0,3	10,4	0,4
11	11,5	595,5	0,1	1679,3	0,3	10,2	0,4
12	12,5	591,9	0,1	1689,5	0,3	10,3	0,4
13	13,5	588,3	0,1	1699,8	0,3	10,2	0,4
14	14,5	584,8	0,1	1710,0	0,3	9,7	0,4
15	15,5	581,5	0,1	1719,7	0,3	9,5	0,4
16	16,5	578,3	0,1	1729,2	0,3	9,9	0,4
17	17,5	575	0,1	1739,1	0,3	8,8	0,4
18	18,5	572,1	0,1	1747,9	0,3	8,9	0,4
19	19,5	569,2	0,1	1756,9	0,3	8,7	0,4
20	20,5	566,4	0,1	1765,5	0,3		

Table 9: Calculated values and uncertainties of ΔG for ν''=2